

Photosensitizers Based on Zinc Phthalocyanine Derivative-Nanoparticles Assemblies

T. POTLOG^{a,*}, I. LUNGU^b AND I. GUTU^a

^aLaboratory of Organic/Inorganic Materials for Optoelectronics, Moldova State University, 60 Al. Mateevici St., MD-2009 Chişinău, Republic of Moldova

^bDoctoral School "Natural Sciences", Moldova State University, 60 Al. Mateevici St., MD-2009 Chişinău, Republic of Moldova

Doi: [10.12693/APhysPolA.146.531](https://doi.org/10.12693/APhysPolA.146.531)

*e-mail: tpotlog@gmail.com

This paper reports the conjugation of (MeIt)₈ZnPcCl₈ to silver nanoparticles (AgNPs) through a metal–ligand coordination system. From the spectral and photophysical studies, the Stokes shift, the excited state lifetime, and the quantum yield are estimated. It was observed that the conjugation of (MeIt)₈ZnPcCl₈ to AgNPs in DMSO/H₂O solution led to an increase in the absorption intensity of the Q band with a maximum at 675 nm and a shift of it of 10 nm. The fluorescence intensity of the (MeIt)₈ZnPcCl₈ is significantly higher than values obtained for (MeIt)₈ZnPcCl₈:AgNP compounds. The presence of AgNPs results in an increase in both triplet quantum yields and lifetimes, which is an advantage in the efficient generation of singlet oxygen quantum yields. The triplet quantum yield of 15.10% for (MeIt)₈ZnPcCl₈ conjugated to AgNP in DMSO/H₂O was obtained (compared to 0.1% for the non-conjugated compound).

topics: ZnPc derivatives, AgNPs, fluorescence, triplet quantum yield

1. Introduction

The use of *metalphthalocyanines* (MPcs) as *photosensitizers* (PSs) in *photodynamic therapy* (PDT) is very advanced due to their photophysical properties. This class of PSs has several significant advantages, e.g., the presence of intense absorption (extinction coefficient of $1.0\text{--}1.5 \times 10^5 \text{ M}^{-1} \text{ cm}^{-1}$) in the red region of the spectrum (600–850 nm) [1–3] and the possibility of introducing substituents into the benzene rings of the macrocycle, as well as its modification, allow for a wide variation in the physicochemical properties of MPcs [4–9]. The penetration of biological tissues in the effective wavelength range of currently used PSs is insignificant, amounting to only a few millimetres. It is known that the most transparent range for the penetration of light into biological tissue is in the far-red and near-*infrared* (IR) region. The development of new PSs that absorb in the far-red region of the spectrum, possessing higher activity and rapid elimination from the body, present a long life of the triplet reactive excited species generated by the photoactive pathways (greater than 500 ns), enough to react with molecular oxygen and induce *reactive oxygen species* (ROS) production, present good solubility and biocompatibility is an urgent task presently. Unfortunately, very often MPcs are hydrophobic species and undergo self-aggregation in aqueous

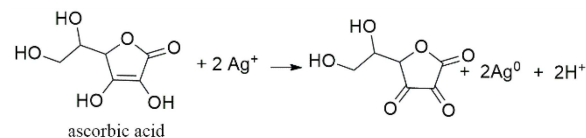


Fig. 1. Reduction of Ag⁺ ions by ascorbic acid.

solutions, which drastically reduces their photosensitizing efficiency. Since the perfect PS does not yet exist, there is still a need to improve the photosensitizing efficiency of PSs or create new PSs with better photosensitizing properties. One solution is to combine MPcs with AgNPs. This study is dedicated to the conjugation of zinc phthalocyanine (ZnPc) derivatives to surface-modified metallic nanoparticles.

2. Materials and methods

2.1. Synthesis of ZnPc derivatives and AgNP colloidal solution

The octakis(chloromethyl) phthalocyanine zinc ((ClMe)₈ZnPc) was obtained by chloromethylation reaction of zinc phthalocyanine [10]. The 50.6 mmol of AlCl₃ is entered into a three-necked flask

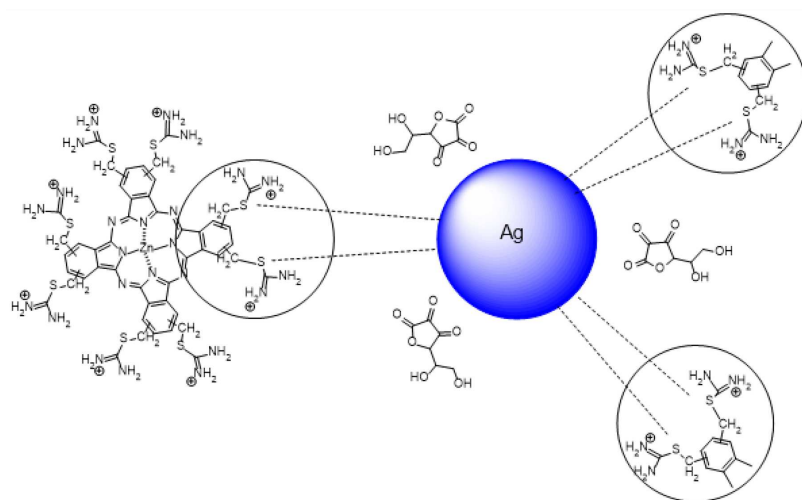


Fig. 2. Scheme of the $(\text{MeIt})_8\text{ZnPcCl}_8\text{-AgNP}$ conjugate.

equipped with a mechanical stirrer and an oil bath. Then, 2 ml of triethylamine is added on cooling. A mixture of 161.5 mmol of paraform and 6.5 ml of thionyl chloride, heated to 75°C , is added slowly to the ZnPc. The mixture is stirred for 6 h at a temperature of 90°C . After this, the mixture is poured onto ice, and the precipitate is separated by filtration and washed on the filter with water and methanol. The product is treated with acetonitrile in a Soxhlet extractor and dried. It results in water-insoluble green powder, slightly soluble in benzene and well soluble in dimethylformamide (DMF), dimethyl sulfoxide (DMSO), and lower alcohols. Based on $(\text{ClMe})_8\text{ZnPc}$, (methyl-isothiuronium) zinc phthalocyanine $(\text{MeIt})_8\text{ZnPcCl}_8$ and the zinc phthalocyanine derivative with eight thiol groups $(\text{HSMe})_8\text{ZnPc}$ were synthesized. The $(\text{ClMe})_8\text{ZnPc}$ reacts easily with thiourea to reflux in ethanol, and $(\text{MeIt})_8\text{ZnPcCl}_8$ is obtained. Under the conditions of a basic hydrolysis of the $(\text{MeIt})_8\text{ZnPcCl}_8$ salt, the thiol derivative results in the acidification of the reaction medium. Due to that, the $(\text{HSMe})_8\text{ZnPc}$ is not soluble in water mixtures, so it was not used in further studies. The silver colloidal nanoparticles (AgNP) are produced by reducing silver nitrate with ascorbic acid and glucose. The scheme of the chemical reaction with ascorbic acid is presented in Fig. 1.

Then, the $(\text{MeIt})_8\text{ZnPcCl}_8$ was conjugated to colloidal AgNPs. Briefly, 2 mg of $(\text{MeIt})_8\text{ZnPcCl}_8$ was dissolved in 2 mL DMSO/ H_2O . Next, the 2 ml of AgNPs colloidal solution for each type was added to the above-mentioned ZnPc derivative solution and stirred for 2 h at 50°C . The mixture was allowed to reflux overnight. The scheme for the $(\text{MeIt})_8\text{ZnPcCl}_8$ conjugate is shown in Fig. 2.

The isothiuronium substituents of Pcs are anchored on the cores through metal-ligand coordination where the weakly bound oxygen-containing ligands (dehydroascorbic acid, gluconic acid) were

partially replaced by Pcs. Silver is well known for its high affinity for S and N and weak affinity to O. Covalent-like strong interactions between the ZnPcs and AgNPs are carried out via the sulfur-by ligand-exchange reaction.

2.2. Characterization techniques

ZnPc, silver nitrate, ascorbic acid, and other chemicals were purchased from Sigma-Aldrich and used without further purification. Infrared absorption spectra were recorded on a Bruker IFS 66s spectrometer. Electronic absorption spectra were recorded on a spectrophotometer Cary 50 UV-Vis (Varian). The steady-state fluorescence spectroscopy was performed using a spectrometer LS55, PerkinElmer Inc., Shelton, CT, USA, equipped with double grating excitation and emission monochromators. Time-correlated single photon counting (TCSPC) technique was used to determine the fluorescence lifetime. The time-resolved fluorescence spectra were recorded on a spectrometer (FLS980, Edinburgh Instruments, Livingston EH54 7DQ, Oxford, UK). All emission decay profiles were determined in a $10 \times 10 \text{ mm}^2$ quartz cell, excited with a xenon lamp as the light source.

3. Results and discussion

3.1. UV-Vis and fluorescence analysis

The ultraviolet-visible (UV-Vis) spectra of the $(\text{MeIt})_8\text{ZnPcCl}_8$, $(\text{MeIt})_8\text{ZnPcCl}_8\text{:AgNP}$ conjugates in DMSO/ H_2O solution and of the silver colloidal nanoparticles (AgNP) are shown in Fig. 3.

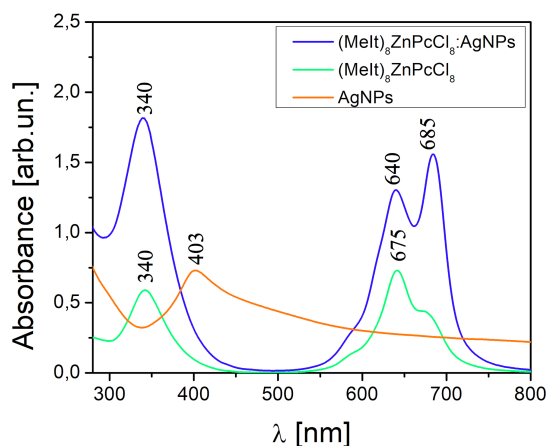


Fig. 3. The UV-Vis spectra of $(\text{MeIt})_8\text{ZnPcCl}_8$ and $(\text{MeIt})_8\text{ZnPcCl}_8:\text{AgNP}$ in DMSO/ H_2O solution and of the silver colloidal nanoparticles (AgNPs).

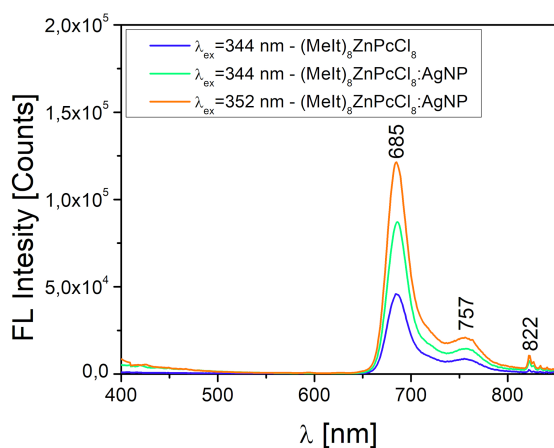


Fig. 4. The fluorescence spectra of $(\text{MeIt})_8\text{ZnPcCl}_8$ and $(\text{MeIt})_8\text{ZnPcCl}_8:\text{AgNP}$ in DMSO/ H_2O solution.

The spectra of $(\text{MeIt})_8\text{ZnPcCl}_8$ and $(\text{MeIt})_8\text{ZnPcCl}_8:\text{AgNP}$ with 1.83×10^{-4} g/ml concentration of the $(\text{MeIt})_8\text{ZnPcCl}_8$ show two bands, the B band situated at 340 nm and the Q band with two distinct peaks in the region 550–800 nm. The Q-band splitting of $(\text{MeIt})_8\text{ZnPcCl}_8$ compounds into two distinct peaks, one with the highest intensity typical for the monomeric 640 nm form of ZnPc and another at 675 nm with lower intensity. For $(\text{MeIt})_8\text{ZnPcCl}_8:\text{AgNP}$ conjugate in the DMSO/ H_2O solvent, the Q band shows the highest intensity peak at 685 nm with a 10 nm shift to the infrared region compared to $(\text{MeIt})_8\text{ZnPcCl}_8$ in the same solvent. AgNPs exhibit a characteristic absorption peak at about 403 nm, which is attributed to surface plasmon excitation. The fluorescence spectra of $(\text{MeIt})_8\text{ZnPcCl}_8$ and $(\text{MeIt})_8\text{ZnPcCl}_8:\text{AgNP}$ in DMSO/ H_2O solution (Fig. 4), excited at 344 nm,

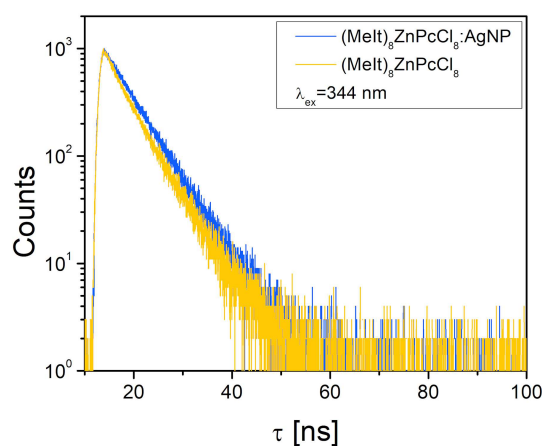


Fig. 5. The fluorescence lifetimes decay of $(\text{MeIt})_8\text{ZnPcCl}_8$ and $(\text{MeIt})_8\text{ZnPcCl}_8:\text{AgNP}$.

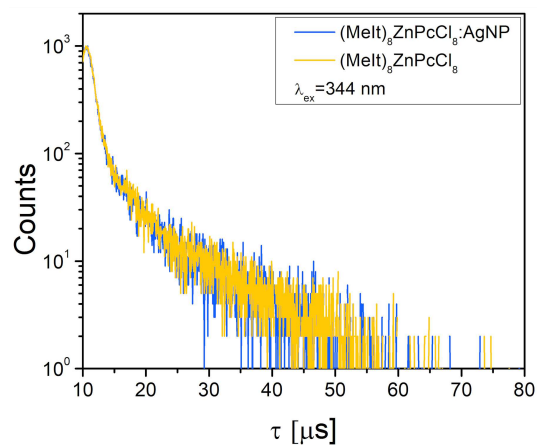


Fig. 6. Triplet-state decay curves of $(\text{MeIt})_8\text{ZnPcCl}_8$ and $(\text{MeIt})_8\text{ZnPcCl}_8:\text{AgNP}$ in DMSO/ H_2O solution.

showed two bands without changing the position of the bands in 650–800 nm region. The same situation is observed in the case of excitation at 352 nm. The spectral positions of these emission bands do not change for excitation wavelengths $\lambda > 352$ nm. The fluorescence intensity of the $(\text{MeIt})_8\text{ZnPcCl}_8$ is significantly higher than values obtained for $(\text{MeIt})_8\text{ZnPcCl}_8:\text{AgNP}$ compounds.

3.2. Fluorescence, phosphorescence lifetimes and quantum yields

The phosphorescence could not be recorded in the compounds analyzed above, probably because there are many deactivation processes that have faster rate constants, such as nonradiative decay and quenching [11, 12]. Figure 5 presents the time a molecule remains in its excited state before returning to the ground state.

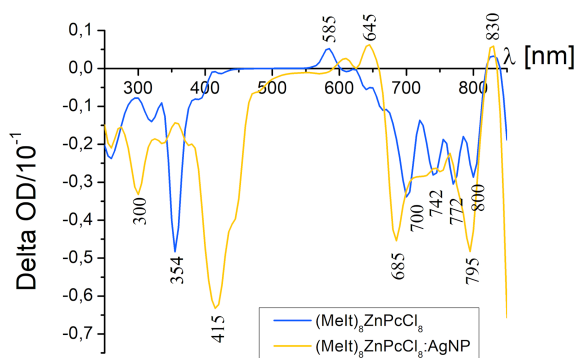


Fig. 7. Transient absorption maps of $(\text{MeIt})_8\text{ZnPcCl}_8$ and $(\text{MeIt})_8\text{ZnPcCl}_8:\text{AgNP}$ in DMSO/ H_2O solution.

The fluorescence decays in Fig. 5 are satisfactorily described by mono exponential functions, suggesting that the solution had only one species that fluoresces. The reduced χ^2 value of near unity was obtained. The τ_F values are 4.6 ns and 5.7 ns for $(\text{MeIt})_8\text{ZnPcCl}_8$ and $(\text{MeIt})_8\text{ZnPcCl}_8:\text{AgNP}$, respectively, and are assigned to relaxation from singlet excited state to ground state. The fluorescence quantum yields (Φ_F) of 0.38% and 1.55% indicate that the compounds exhibit relatively low quantum efficiency.

The values of Φ_F for $(\text{MeIt})_8\text{ZnPcCl}_8$ and $(\text{MeIt})_8\text{ZnPcCl}_8:\text{AgNP}$ in DMSO/ H_2O are smaller than for ZnPc. The triplet decay curves of $(\text{MeIt})_8\text{ZnPcCl}_8$ and $(\text{MeIt})_8\text{ZnPcCl}_8:\text{AgNP}$ in DMSO/ H_2O are shown in Fig. 6. The decay curves exhibit bi-exponential behaviour with fluorescence lifetimes of 1.02, 8.42, 1.13, and 9.43 μs , respectively.

The presence of two lifetimes in $(\text{MeIt})_8\text{ZnPcCl}_8$ and $(\text{MeIt})_8\text{ZnPcCl}_8:\text{AgNP}$ in DMSO/ H_2O could be explained in terms of quenched and unquenched fluorescence lifetime for the ZnPc derivative [13]. The fluorescence lifetime is longer for the conjugate than for the $(\text{MeIt})_8\text{ZnPcCl}_8$ alone. The triplet quantum yields of 15.10% for $(\text{MeIt})_8\text{ZnPcCl}_8$ conjugate to AgNP in DMSO/ H_2O were reached. The AgNP showed a modest improvement in photophysical parameters.

3.3. Transient absorption spectroscopy

The transient absorption (TA) study was done by exciting the molecule of synthesized compounds at 355 nm. The transient absorption spectra of $(\text{MeIt})_8\text{ZnPcCl}_8$ and $(\text{MeIt})_8\text{ZnPcCl}_8:\text{AgNP}$ in DMSO/ H_2O shown in Fig. 7 displayed some differences.

TA spectra show both positive and negative features due to the difference between the ground-state absorption, A_{probe} , and that of the excited

state, $A_{\text{pump+probe}}$, at a given time delay between the two pulses. The weakly positive bands are assigned to $T_1 - T_n$ absorption. Metallic nanoparticles such as Au and Ag are known to quench the MPc fluorescence due to energy transfer from phthalocyanines in the excited state to the silver nanoparticles [14]. A strong ground state bleach appears at 354 nm for $(\text{MeIt})_8\text{ZnPcCl}_8$, while for the $(\text{MeIt})_8\text{ZnPcCl}_8:\text{AgNP}$ it is shifted to 415 nm, which corresponds to the surface plasmon absorption of nanoparticles. The maxima in the range of 685–800 nm for $(\text{MeIt})_8\text{ZnPcCl}_8:\text{AgNP}$ are assigned to the isothiouonium substituents of Pcs anchored on the cores through metal–ligand coordination, where the weakly bound oxygen-containing ligands are partially replaced by Pcs. The bleaching at 685 nm and 795 nm corresponds to the ground state (S_0) absorption of $(\text{MeIt})_8\text{ZnPcCl}_8$ in DMSO/ H_2O . This confirms the weak electron transfer from the excited state of $(\text{MeIt})_8\text{ZnPcCl}_8$ to the AgNP nanoparticle conduction band.

4. Conclusions

This paper describes the effect of silver nanoparticles on the photophysical behaviour of the $(\text{MeIt})_8\text{ZnPcCl}_8$. It was found that the presence of AgNPs quenched the fluorescence of the $(\text{MeIt})_8\text{ZnPcCl}_8:\text{AgNP}$ in the hybrid system. However, the presence of AgNPs enhanced the triplet lifetime and triplet quantum yield of the synthesized phthalocyanines by the weak electron transfer from the excited state of $(\text{MeIt})_8\text{ZnPcCl}_8$ to the AgNP nanoparticle conduction band.

Acknowledgments

This research paper was financially supported by the Ministry of Education and Research of the Republic of Moldova, subprogram “Design of supramolecular architectures based on metal phthalocyanine derivatives — functionalized nanoparticles for medicine”, #011209.

References

- [1] M. Brust, M. Walker, D. Bethell, D. Schiffrin, R. Whyman, *J. Chem. Soc., Chem. Commun.* **7**, 801 (1994).
- [2] X. Chen, Q. Ye, D. Ma, J. Chen, Y. Wang, H. Yang, *J. Lumin.* **195**, 348 (2018).
- [3] H.-B. Cheng, X. Li, N. Kwon, Y. Fang, G. Baek, G. Yoon, *J. Chem. Commun.* **55**, 12316 (2019).

- [4] O.V. Dementeva, M.M. Vinogradova, E.A. Lukyanets, L.I. Soloveva, V.A. Ogarev, V.M. Rudoy, *Colloid J.* **76**, 53945 (2014).
- [5] E. Dube, N. Nwaji, J. Mack, T. Nyokong, *New J. Chem.* **42**, 14290 (2018).
- [6] E. Dube, T. Nyokong, *J. Mol. Struct.* **1181**, 312 (2019).
- [7] K. Kang, J. Wang, J. Jasinski, S. Achilefu, *J. Nanobiotechnol.* **9**, 16 (2011).
- [8] N. Masilela, T. Nyokong, *J. Photochem. Photobiol. A* **223**, 124 (2011).
- [9] N. Nwahara, M. Managa, E. Prinsloo, T. Nyokong, *ChemistrySelect* **4**, 9084 (2019).
- [10] I. Guțu, V. Suman, A. Barbă, T. Potlog, in: *6th Int. Conf. on Nanotechnologies and Biomedical Engineering (ICNBME 2023)*, Vol. 91, Springer, Cham 2023.
- [11] A. Ogunsipe, J.-Y. Chen, T. Nyokong, *New J. Chem.* **28**, 822 (2004).
- [12] N. Rapulenyane, E. Antunes, T. Nyokong, *New J. Chem.* **37**, 1216 (2013).
- [13] J. Widoniak, S. Eiden-Assmann, G. Maret, *Colloids Surf. A* **270–271**, 340 (2005).
- [14] R. Garifullin, T.S. Erkal, S. Tekin, B. Ortac, A. Gul Gurek, V. Ahsen, H. Gul Yaglioglu, A. Elmali, M.O. Guler, *J. Mater. Chem.* **22**, 2553 (2012).